articles

A computational role for slow conductances: single-neuron models that measure duration

Scott L. Hooper, Einat Buchman and Kevin H. Hobbs

Neuroscience Program, Department of Biological Sciences, Ohio University, Athens, Ohio 45701 USA

Correspondence should be addressed to S.L.H. (hooper@ohio.edu)

Humans effortlessly interpret speech and music, whose patterns can contain sound durations up to thousands of milliseconds. How nervous systems measure such long durations is unclear. We show here that model neurons containing physiological slow conductances are 'naturally' sensitive to duration, replicate known duration-sensitive neurons and can be 'tuned' to respond to a wide range of specific durations. In addition, these models reproduce several other properties of duration-sensitive neurons not selected for in model construction. These data, and the widespread presence of slow conductances in nervous systems, suggest that slow conductances might play a major role in duration measurement.

To understand the problems the nervous system faces in analyzing speech and music, consider the song 'Y.M.C.A.' (**Fig. 1**). Two measures of the song's chorus are shown both in musical notation (line 1) and in an alternative representation in which rectangles denote the time and duration of each note (lines 2–4). The song's beat, a repeating series of bass drum (~90 Hz) eighth notes, is shown only in the rectangle representation (line 5); this is the rhythm people dance to. Almost all the song's information is contained in the non-repetitive sequence of long-duration sounds (in the original recorded version of 'Y.M.C.A', eighth notes last 250, quarter notes 500 and half notes 1,000 ms) that comprises the song's melody (lines 2–4). This property—that most information is carried in complex sequences of long-duration sounds—is present in many auditory signals, and especially in speech and music. Extracting information from these signals requires measuring long durations; in the studies described here we investigated the neural mechanism underlying this ability.

Neurons that fire after sounds of specific durations are present in amphibian midbrain[1,2] and mammalian inferior colliculus, thalamus and cortex[3–5]. Three types of duration-sensitive neuron are known: low-pass (which fire after durations shorter than a certain value), high-pass (which fire after durations longer than a certain value) and band-pass neurons (which fire only after durations within a narrow range)[3–5]. These neurons respond to durations of 2–75 ms in bat[3] and up to 200 ms in cat[5]. Whether similar neurons are present in humans is unknown, but interpreting speech and music would require neurons sensitive to durations up to thousands of milliseconds. Sound inhibits duration-sensitive neurons[6], and duration sensitivity has been proposed to arise because the coincidence of post-inhibitory rebound and delayed excitatory synaptic input drives the neurons above spike threshold[3,6–9]. For short sounds (<50 ms), axonal and synaptic delays could produce the delays in excitatory input this hypothesis requires, but these mechanisms are inadequate to produce the delays required to measure longer durations[6].

We present a hypothesis that obviates the need for delayed synaptic excitation. We propose that duration-sensitive neurons possess currents that slowly change during sound-induced inhibition, and the neurons therefore fire only after certain sound durations. Models that reproduce the three types of duration-sensitive neurons can be constructed using physiological slow conductances. Furthermore, although this was not a goal of our model construction, these models also reproduce several other properties of duration-sensitive neurons not selected for in model construction.

RESULTS

To test the ability of slow conductances to produce duration-sensitive neurons, we created single-compartment models of neurons having I_{Na} and IK_D and (depending on the model) the transient K current I_A, the hyperpolarization-activated, depolarizing current I_h and the low-threshold Ca current I_T. The inhibition duration-sensitive neurons receive during sound[6] was modeled with a synaptic current open throughout sound duration.

Interaction of IK_D and I_A can create low-pass models (**Fig. 2a**). When the model was hyperpolarized for 2, 125, 250, 375, 500, 625, 750, 875 and 1,000 ms, it fired after all hyperpolarizations ≤500 ms; in the auditory system it would fire for all sounds ≤500 ms. Model duration sensitivity arises as follows. At rest, sufficient IK_D is open to prevent firing, and I_A is almost completely inactivated. Hyperpolarization quickly closes IK_D but only slowly removes I_A inactivation (at –80 mV, the time constant of I_A inactivation removal is 500 ms). After short hyperpolarizations, little I_A is available to open, and sufficient IK_D closes to induce post-inhibitory rebound and firing. As duration increases, more I_A inactivation is removed (bottom trace) and eventually I_A blocks firing. Models tuned to durations from 2 to 1,800 ms, which span the durations in speech and music, can be constructed using physiological I_A parameters[10–14].

I_h can create high-pass models (**Fig. 2b**). When this model was hyperpolarized for the same durations as in **Figure 2a**, it fired
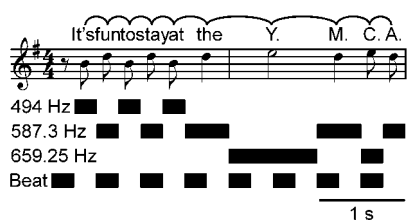
Fig. 1. 'Y.M.C.A' temporal pattern. Line 1 shows the sound pattern in musical notation. The pattern consists of five alternations of B and D eighth notes, a quarter note of D, a half note of E, a quarter note of D and two E and D eighth notes (B above middle C, 494 Hz; D, 587.3 Hz; E, 659.25 Hz). Lines 2–4 are an alternate representation in which the rectangles represent note duration. Line 5 is the song's beat (eighth notes separated by eighth note rests) in the rectangle representation. 'Y.M.C.A.' was composed by J. Morali, H. Belolo and V. Willis and performed by the Village People.

after all durations ≥500 ms. In this model little IK_D is open at rest, and there is therefore no post-inhibitory rebound due to IK_D closing. Instead I_h supports post-inhibitory rebound, and the model fires only after durations long enough to activate sufficient I_h to drive the model above threshold. I_h is present in many vertebrate neurons[15], including those of the auditory system[16,17]. Models tuned to durations from 15 to >5,000 ms can be constructed using physiological I_h parameters[10,11,18,19].

I_A and I_h can create band-pass models (**Fig. 2c**). When this model was hyperpolarized for the same durations as in **Figure 2a**, and also for 480 and 522 ms, it fired only for durations narrowly centered around 500 ms. The model contains I_A and I_h currents with the same kinetics as in **Figure 2a** and **b**. I_h increases with duration, and eventually the model fires. As duration increases further, enough I_A inactivation is removed that I_A overcomes I_h and the model no longer reaches threshold. Models tuned to center durations from 50 to 3,000 ms can be constructed using phys-

iological I_A and I_h parameters. Models tuned to shorter durations can be constructed using faster I_h-like currents[20] or delay line mechanisms, which are biologically possible for short durations.

Duration-sensitive neurons can fire short spike bursts, and slow conductance–based low-, high- and band-pass bursting models can be constructed (**Fig. 2d–f**). We obtained a low-pass burst model (**Fig. 2d**) by slightly (≤10%) hyperpolarizing the voltage dependence of the opening and closing rates of IK_D (ref. 21). In the absence of I_A, any duration of hyperpolarization induces the model to fire a short spike burst at the end. Varying I_A amplitude tunes the model to fire only for durations shorter than a certain value. Bursting in the other models (**Fig. 2e, f**) was supported by I_T, from which hyperpolarization removes inactivation. Tuning in the high-pass model was achieved with an I_A whose inactivation removal was faster than that for I_T but which, when I_A and I_T were fully activated, could not prevent I_T from inducing a burst. I_A thus blocks firing after short hyperpolarizations but not long ones. The band-pass model was tuned by adding a second, slower I_A that blocked firing after long hyperpolarizations; the two I_As constrained firing to a short duration range. Altering conductance amplitude and kinetics changes burst spike number and model tuning; the models can be physiologically tuned through the same ranges as single-spike models.

All three models fired fewer spikes as they approach their firing limit(s); this decline also occurs in bursting duration–sensitive neurons[4,5]. In slow-conductance models, this decline is a 'natural' consequence of the mechanisms underlying model tuning. For instance, in the bursting low-pass model, the growth of I_A eventually blocked firing; this same growth, by partially offsetting the post-inhibitory rebound, also resulted in the model firing fewer spikes at intermediate durations. Similar I_A-mediated decreases in post-inhibitory rebound occur in dorsal cochlear nucleus pyramidal neurons[22].

Tones are often repeated with brief inter-tone (silent) intervals. To respond correctly to repeated tones, duration-sensitive neurons require inter-tone intervals of 30–200 ms[23]; the models in **Figure 2** required intervals of 60–400 ms. However, the currents in these models all had the same kinetics (only conductance amplitude was varied). When conductance kinetics was also varied (but always in the physiological range), the models responded correctly to repeated tones with inter-tone intervals of 10–60 ms.

In human perception, the accuracy of duration measurement decreases linearly with duration, and is ±5% of center duration[24]. That is, durations between 475 and 525 ms (range 50 ms) cannot be distinguished from 500 ms (center duration), and durations between 950 and 1,050 ms (range 100 ms) cannot be distinguished from 1,000 ms (center duration). This is also seen in band-pass neurons: neurons tuned to short durations fire over a narrower duration range than neurons tuned to long durations[8]. Response range similarly increased with tuned duration in both our single-spike (**Fig. 3a–c**; when the model was tuned to 0.25, 0.5 and 1 s, its response ranges were 19, 42 and 81 ms, respectively) and bursting (**Fig. 3d** and **e**) band-pass models.
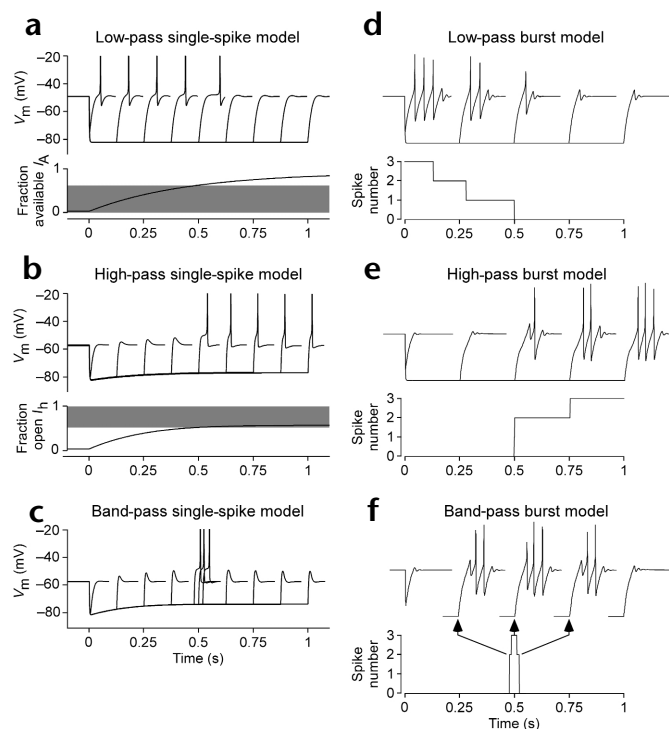

Fig. 2. Models that reproduce low-, high- and band-pass neurons. Left column, single-spike models; right column, bursting models. In all panels, top traces are model responses to hyperpolarizations of various durations. (**a, d**) Low-pass models, with firing for all durations ≤500 ms (**b, e**) High-pass models, with firing for all durations ≥500 ms; (**c, f**), band-pass models, with firing for a narrow range of durations centered around 500 ms. Lower traces in (**a**) and (**b**) are fraction of available I_A and open I_h in response to sustained hyperpolarization; gray rectangles are values for which the model can fire. Plots in (**d**), (**e**) and (**f**) show spike number as a function of duration.
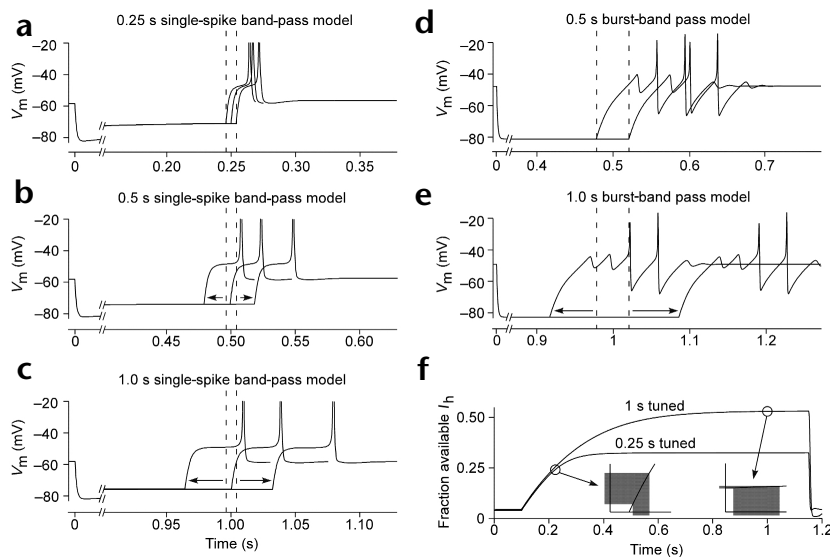
Fig. 3. Band-pass model response range increases with tuned duration. Single-spike models: (**a**) tuned to 0.25 s, response range 0.241–0.26 s; (**b**) tuned to 0.5 s, response range 0.480–0.522 s; (**c**) tuned to 1 s, response range 0.966–1.047 sec. (**d**, **e**) Similar data for bursting models (for clarity, only the ranges over which the models fire two spikes are shown; one-spike ranges are slightly larger). Dashed lines are response ranges of 0.25 s single-spike (**a**–**c**) and 0.5 s burst (**d**, **e**) models. The response ranges become larger (**f**) because the curves governing current expression flatten as duration increases. Curves represent available I_h fraction during a 1.03 s hyperpolarization for 0.25 s and 1 s single-spike models. Insets are expansions of the curves near the fraction where the models can fire; insets have equal available I_h fraction ($\Delta = 0.0231$) and time ($\Delta = 66$ ms) ranges. The horizontal gray rectangles show the fraction range in which each model can fire; the vertical gray rectangles show the corresponding time range. Although the 0.25 s model can fire over a much wider available I_h range, because of the steepness of its curve in this region, this corresponds to a much shorter time range. The two curves do not achieve the same fraction at long times because, as a result of the different I_A and I_h maximal conductances in them, their voltages differ in the later portions of the hyperpolarizations.

This increased response range 'naturally' arises in slow-conductance models. The models fire when their currents simultaneously have values within certain windows. Tuning is achieved by adjusting conductance maxima until, at the tuned duration, all currents have values within these windows. The fraction of available or open current rises as a function of $1 - e^{t/c}$. As the models are tuned to longer durations, their firing occurs further in flatter regions of these curves, and a given current window corresponds to longer time windows. Thus, during a sustained hyperpolarization, the 0.25 s single-spike band-pass model fired for fractions of available I_h between 0.2602 and 0.2756, whereas the 1 s single-spike band-pass model fired for fractions between 0.5291 and 0.5298 (**Fig. 3f**). Although the I_h fraction range over which firing can occur was 22-fold greater in the 0.25 s model, because of the steepness of its curve in this region, the duration range to which this I_h fraction range corresponded was much narrower in the 0.25 s model than in the 1 s model.

DISCUSSION

It is important to compare our models to experimental data. First, sounds occur at different intensities, and the tuning of duration-sensitive neurons can vary or not with changes in sound intensity[4,5,25]. Because slow-conductance activation and inactivation are voltage dependent, changing hyperpolarization amplitude changes the tuning of slow-conductance models. Slow-conductance models can therefore reproduce, depending on the nature of their synaptic input, both sound intensity–independent and –dependent neurons. Intensity-independent models have synaptic input that does not vary with intensity, or a synapse so strong that it reaches reversal potential for all inputs. Intensity-dependent models have synaptic input that varies with intensity, and a synapse weak enough that postsynaptic hyperpolarization varies with changes in presynaptic activity.

Second, auditory midbrain neurons display duration tuning under voltage-clamp recording conditions[3,7]. Because our models rely on voltage-dependent conductances, these data appear to contradict the slow-conductance hypothesis. However, good space

clamp cannot be obtained in these neurons[3,7] (E. Covey, personal communication). This problem can be resolved by hyperpolarizing duration-sensitive neurons to test whether they show rebound firing and whether spike number varies with hyperpolarization duration. To our knowledge, such experiments have not been reported, but about one-third of the neurons in rat inferior colliculus slices rebound and spike after square-wave hyperpolarization[26].

Third, consistent with the slow-conductance hypothesis, which depends on hyperpolarization, inhibitory transmitter antagonists abolish duration sensitivity[9]. Because the delayed synaptic excitation hypothesis also requires inhibition, these data do not distinguish between the hypotheses. An experiment that would do so would be one blocking excitatory synaptic input. However, as a multisynaptic pathway mediates sound-evoked responses[6], this test may be impossible to perform. In addition, the slow-conductance and synaptic hypotheses are not mutually exclusive; both mechanisms could be present and have complementary roles in duration sensing, with slow conductance mechanisms becoming increasingly important as duration increases.

Fourth, auditory neurons have currents similar to those used here. Some inferior colliculus neurons contain IK_D currents with altered activation-voltage dependencies[27], as in our single-spike and burst low-pass models. A slow I_h is present in cochlear nucleus octopus cells[17], and slow I_A and I_T are present in some inferior colliculus neurons; the latter neurons show post-inhibitory rebound firing[27]. Unfortunately, in the inferior colliculus work, duration sensitivity could not be examined, and direct comparison with our models is thus impossible. Nonetheless, these data show that the fundamental building blocks of our models are present in auditory neurons.

Slow-conductance band-pass neurons can analyze the 'Y.M.C.A.' melody (**Fig. 4**). For the note B (494 Hz; **Fig. 4a**), the 0.25 s neuron fires at 0.25, 0.75 and 1.25 s, and thereby signals that immediately before these times a 494 Hz eighth note occurred (because there are no 494 Hz quarter or half notes, the 0.5 s and 1 s neurons do not fire). For the note D (587.3 Hz; **Fig. 4b**), firing of the 0.25 s or 0.5 s neurons signals when 587.3 Hz eighth or
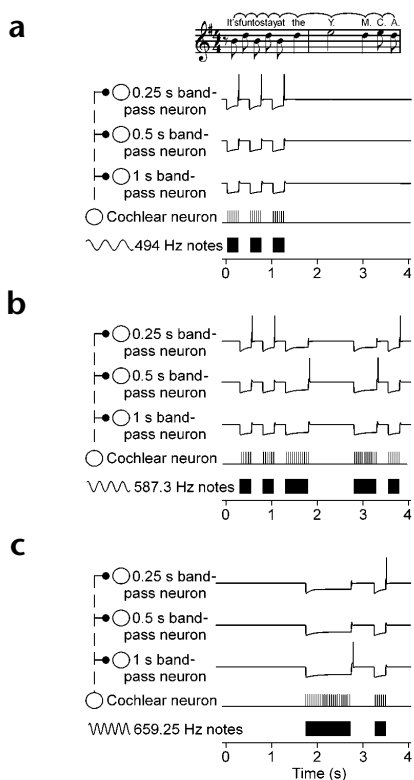
a

○ 0.25 s band-pass neuron
○ 0.5 s band-pass neuron
○ 1 s band-pass neuron
○ Cochlear neuron
494 Hz notes

0 1 2 3 4

b

○ 0.25 s band-pass neuron
○ 0.5 s band-pass neuron
○ 1 s band-pass neuron
○ Cochlear neuron
587.3 Hz notes

0 1 2 3 4

c

○ 0.25 s band-pass neuron
○ 0.5 s band-pass neuron
○ 1 s band-pass neuron
○ Cochlear neuron
659.25 Hz notes

0 1 2 3 4

Time (s)

Fig. 4. Analysis of 'Y.M.C.A.' using single-spike slow-conductance band-pass neurons. Bottom trace (in each panel), sound pattern of note; next trace up, firing of a cochlear neuron tuned to that note; three upper traces, activities of 1, 0.5 and 0.25 s band-pass neurons inhibited when tones of 494 (**a**), 587.3 (**b**), and 659.25 (**c**) Hz are played. In (**a**), firing of 0.25 s neuron signals that 494 Hz (B in musical notation) eighth notes occurred immediately before 0.25, 0.75 and 1.25 s. In (**b**), firing of 0.25 s neuron signals that 587.3 Hz (D) eighth notes occurred immediately before 0.5, 1 and 3.75 s; firing of 0.5 s neuron signals that 587.3 Hz quarter notes occurred immediately before 1.75 and 3.25 s. In (**c**), firing of 0.25 s neuron signals that a 659.25 Hz (E) eighth note occurred immediately before 3.5 s; firing of 1 s neuron signals that a 659.25 Hz half note occurred immediately before 2.75 s. Connections between cochlear and band-pass neurons are dashed because these connections are multisynaptic[6].

were multiplied by $3^{(37-23.5)/10} = 3.54$). When necessary for tuning, conductance kinetics was adjusted by multiplying da/dt and db/dt by constants (all changes were in the physiological range). For I_{Na} and IK_D, $a_\infty = \alpha/(\alpha + \beta)$ and $\tau_a = 1/(\alpha + \beta)$, where α and β are membrane voltage (V_m)–dependent opening and closing rates[35]. I_A, I_h and I_T a_∞, b_∞, τ_a and τ_b were given by equations of the form:

$$a_\infty = 1/(1 + e^{(V_m - V_{1/2})/S}) \text{ and } \tau_a = c/(e^{(V_m - V_{1/2\tau1})/S_{\tau1}} + e^{(V_m - V_{1/2\tau2})/S_{\tau2}})^{36}.$$

The currents were calculated from $I = \bar{g}a^{n_1}b^{n_2}(V_m - E)$ or $I = \bar{P}a^{n_1}b^{n_2}G(V_m,[Ca_o],[Ca_i])$, where $\bar{g}$ is maximum conductance, E reversal potential, $\bar{P}$ maximum permeability, $[Ca_o]$ and $[Ca_i]$ external and internal Ca concentration and G the constant field equation. V_m was given by $dV_m/dt = $ [injected current $- \Sigma$(membrane and synaptic currents)]$/C_m$, where C_m is membrane capacitance (0.29 nF in all simulations). Models were implemented in ModelMaker (FamilyGenetix, Oxford, UK; fourth-order Runge-Kutta integration, accuracy 0.0001, error 0.001) or Simulink/Matlab (Mathworks, Natick, Massachusetts; ODE45 Dormand-Prince integration, relative tolerance 10^{-4}; absolute tolerance 10^{-5}).

Model equations (except for I_T, τ is in ms, V_m in mV, I in nA and $\bar{g}$ in μS) were as follows:

$$I_{syn} + \bar{g}_{syn}(V_m + 85); \ \bar{g}_{syn} = 0.2 \text{ during sound and 0 otherwise}$$

$$I_{leak} = \bar{g}_{leakK} \cdot (V_m + 105) + \bar{g}_{leakNa} \cdot (V_m - 45)$$

$$I_{Na} = \bar{g}_{Na} \cdot m^3 \cdot h \cdot (V_m - 45)$$

$$\alpha_m = 0.091 \cdot (V_m + 38)/(1 - e^{-(V_m + 38)/5});$$

$$\beta_m = -0.062 \cdot (V_m + 38)/(1 - e^{(V_m + 38)/5})$$

$$\alpha_h = 0.016 \cdot e^{-(V_m + 55)/15}; \ \beta_h = 2.07/(1 + e^{-(V_m - 17)/21})$$

$$I_{K_D} = \bar{g}_{K_D} \cdot n^4 \cdot (V_m + 105)$$

$$\alpha_n = 0.01 \cdot (V_m + 45)/(1 - e^{-(V_m + V_{1/2K_D}\alpha)/5});$$

$$\beta_n = 0.17 \cdot e^{-(V_m + V_{1/2K_D}\beta)/40}$$

Single-spike models, $V_{1/2K_D}\alpha = -45$, $V_{1/2K_D}\beta = -50$

Burst models, $V_{1/2K_D}\alpha = -47.5$, $V_{1/2K_D}\beta = -55$

$$I_h = \bar{g}_h \cdot a_h \cdot (V_m + 30)$$

$$a_{\infty h} = 1/(1 + e^{(V_m + 75)/5.5});$$

$$\tau_{a h} = 270/(e^{-(V_m + 90)/12.5} + e^{(V_m + 75)/5})$$

quarter notes sound. For the note E (659.25 Hz; **Fig. 4c**), firing of the 0.25 s or 1 s neurons signals when 659.25 Hz eighth or half notes sound. The model thus transforms the 'Y.M.C.A.' melody into a duration-based place map in which the firing of specific neurons signals the time and duration of each note.

The brain's analysis of the beat line (**Fig. 1**) remains to be explained. The beat conveys only repeat period (the song's tempo) and relative duration (that beat duration is, in this case, 50% of repeat period—eighth notes separated by eighth rests). One possibility is that higher centers calculate these measures (by unknown mechanisms) using input from beat-excited duration-sensitive neurons. We have shown elsewhere, however, that neurons with slow membrane properties vary their firing as a function of beat parameters and can identify all repeating on/off patterns such as beat lines[28], and that slow-conductance models reproduce these data (E.B., J.B. Thuma, A.L. Weaver, and S.L.H., *Soc. Neurosci. Abstr.* **26**, 748.9, 2000).

These data and those presented here thus show that, in theory, all temporal aspects of music, speech and other, similar patterns can be analyzed by slow-conductance neurons. That individual cells can 'measure' temporal patterns is further supported by work showing pattern-specific variation in second-messenger concentration, protein and gene expression, membrane conductance levels, firing delay and peptide secretion in isolated cells or cell groups driven by varying temporal input[29–34]. Taken together, this work suggests that individual neurons can perform relatively complicated temporal analyses, and that slow conductances may be centrally involved in this process.

METHODS

Conductance activation a (or inactivation, b) was given by $da/dt = (a_\infty - a)/\tau_a$, where a_∞ is steady-state activation and τ_a is the activation time constant. da/dt and db/dt were temperature compensated using $Q_{10} = 3$ (data were acquired at 23.5°C and models run at 37°C, so da/dt and db/dt

articles

© 2002 Nature Publishing Group http://neurosci.nature.com

nature *neuroscience* • volume 5 no 6 • june 2002

555

$$I_A = \bar{g_A} \cdot a_A{}^3 b_A \cdot (V_m + 105)$$

$$a_{\infty A} = 1/(1 + e^{-(V_m - V_{1/2 I_A a_\infty})/20});$$

$$\tau_{aA} = 0.37 + 1/(e^{(V_m + 35.8)/19.7} + e^{-(V_m + 79.7)/12.7})$$

Single-spike models, $V_{1/2 I_A a_\infty} = -26$

Burst models, $V_{1/2 I_A a_\infty} = -36.$

$$b_{\infty A} = 1/(1 + e^{(V_m + 68)/s_{I_A b_\infty}});$$

$$\tau_{bA} = \begin{cases} 20 & V_m \geq -80 \\ 500/(e^{(V_m + 60)/2} + e^{-(V_m + 80)/20}) & V_m < -60 \end{cases};$$

Single-spike models, $S_{I_A b_\infty} = 6$; burst models, $S_{I_A b_\infty} = 4.$

I_{A_1}, τ_a and τ_b were multiplied by 3 in the burst low- and band-pass models and by 1.67 in burst high-pass models. I_{A_2}, τ_a and τ_b were multiplied by 10 in the burst band-pass models.

$$I_T = \bar{P_{Ca}} \cdot a_T{}^2 \cdot b_T \cdot \frac{z^2 F^2 V_m}{RT} \cdot \left([Ca_i] - [Ca_o] e^{\frac{-zFV_m}{RT}} \right) \bigg/ \left(1 - e^{\frac{-zFV_m}{RT}} \right)$$

$$a_{\infty T} = 1/(1 + e^{-6.2});$$

$$\tau_{aT} = 0.612 + 1/(e^{(V_m + 13.6)/-16.7} + e^{(V_m + 16.8)/18.2})$$

$$b_{\infty T} = 1/(1 + e^{(V_m + 84.5)/4.03});$$

$$\tau_{bT} = \begin{cases} e^{(V_m + 467)/66.6} & V_m < -80 \\ 28 + e^{(V_m + 21.88)/-10.52} & V_m \geq -80 \end{cases}$$

In the I_T equation, $\bar{P}$ is in nanoliters/s, z is valence (2), F is Faraday's constant (9.6×10^4 coulomb (C)/mol), V_m is in volts, R is the gas constant (8.31 J/K mol), T is temperature in K, $[Ca_i]$ and $[Ca_o]$ are in mol/liter (M), and therefore I is in nA. V_m is in mV in the $a_{\infty T}$, τ_{aT}, $b_{\infty T}$ and τ_{bT} equations. Both I_T τ values were multiplied by 1.2. I_T changed $[Ca_i]$ as follows: 1 nA = (10^{-9} C/s) × (10^{-3} s/ms) × (1 mol_{charge}/9.6 × 10^4 C) × (1 mol_{Ca}/2 mol_{charge}) = 5.18×10^{-18} mol_{Ca}/ms. Neurons had a membrane area of 2.9×10^{-4} cm^2. Assuming that Ca variation was limited to a 100 nm shell under the membrane, shell volume was 2.9×10^{-4} cm^2 × 100 nm × (10^{-7} cm/nm) × (10^{-3} liter/cm^3) = 2.9×10^{-12} liter (shell width is small enough that the fact that the cell is spherical can be ignored). Therefore, 1 nA = (5.18×10^{-18} mol_{Ca}/ms)/2.9×10^{-12} liter = 1.79×10^{-6} M/ms. $[Ca_i]$ was calculated from $d[Ca_i]/dt = I_T \times (1.79 \times 10^{-6}$ M/ms nA) + $([Ca_{i\infty}] - [Ca_i])/\tau_{Cai}$, where $[Ca_{i\infty}] = 3 \times 10^{-8}$ M and τ_{Cai} = 2 ms. Model maximum conductances are given in Supplementary Table 1 online.

Note: Supplementary information is available on the Nature Neuroscience website.

Competing interests statement

The authors declare that they have no competing financial interests.

1. Potter, H. D. Patterns of acoustically evoked discharges of neurons in the mesencephalon of the bullfrog. *J. Neurophysiol.* **28**, 1155–1184 (1965).
2. Hall, J. & Feng, A. S. Neural analysis of temporally patterned sounds in the frog's thalamus: processing of pulse duration and pulse repetition rate. *Neurosci. Lett.* **63**, 215–220 (1996).
3. Casseday, J. H., Ehrlich, D. & Covey E. Neural tuning for sound duration: role of inhibitory mechanisms in the inferior colliculus. *Science* **264**, 847–850 (1994).
4. Galazyuk, A. V. & Feng, A. S. Encoding of sound duration by neurons in the auditory cortex of the little brown bat, *Myotis lucifugus*. *J. Comp. Physiol. A* **180**, 301–311 (1997).
5. He, J., Hashikawa, T., Ojima, H. & Kinouchi, Y. Temporal integration and duration tuning in the dorsal zone of cat auditory cortex. *J. Neurosci.* **17**, 2615–2625 (1997).
6. Covey, E. & Casseday, J. H. Timing in the auditory system of the bat. *Annu. Rev. Physiol.* **61**, 457–476 (1999).
7. Covey, E., Kauer, J. A. & Casseday, J. H. Whole-cell patch-clamp recording reveals subthreshold sound–evoked postsynaptic currents in the inferior colliculus of awake bats. *J. Neurosci.* **16**, 3009–3018 (1996).
8. Ehrlich, D., Casseday, J. H. & Covey, E. Neural tuning to sound duration in the inferior colliculus of the big brown bat, *Eptesicus fuscus*. *J. Neurophysiol.* **77**, 2360–2372 (1997).
9. Casseday, J. H., Ehrlich, D. & Covey, E. Neural measurement of sound duration: control by excitatory inhibitory interactions in the inferior colliculus. *J. Neurophysiol.* **84**, 1475–1487 (2000).
10. Golowasch, J. & Marder, E. Ionic currents of the lateral pyloric neuron of the stomatogastric ganglion of the crab. *J. Neurophysiol.* **67**, 318–331 (1992).
11. Huguenard, J. R. & McCormick, D. A. Simulation of the currents involved in rhythmic oscillations in thalamic relay neurons. *J. Neurophysiol.* **68**, 1373–1383 (1992).
12. Lopez-Lopez, J. R., DeLuis, D. A. & Gonzalez, C. Properties of a transient K$^+$ current in chemoreceptor cells of rabbit carotid body. *J. Physiol.* **460**, 15–32 (1993).
13. Wang, W. Y., McKenzie, J. S. & Kemm, R. E. Whole-cell K$^+$ currents in identified olfactory bulb output neurones of rats. *J. Physiol.* **490**, 63–77 (1996).
14. Buckingham, S. D. & Spencer, A. N. K$^+$ currents in cultured neurones from a polyclad flatworm. *J. Exp. Biol.* **203**, 3189–3198 (2000).
15. Pape, H. C. Queer current and pacemaker: the hyperpolarization-activated cation current in neurons. *Annu. Rev. Physiol.* **58**, 299–327 (1996).
16. Chen, C. Hyperpolarization-activated current (I_h) in primary auditory neurons. *Hear. Res.* **110**, 179–190 (1997).
17. Bal, R. & Oertel D. Hyperpolarization-activated, mixed-cation current (I_h) in octopus cells of the mammalian cochlear nucleus. *J. Neurophysiol.* **84**, 806–817 (2000).
18. Hutcheon, B., Miura, R. M. & Puil, E. Models of subthreshold membrane resonance in neocortical neurons. *J. Neurophysiol.* **76**, 698–714 (1996).
19. Angstadt, J. D. Persistent inward currents in cultured Retzius cells of the medicinal leech. *J. Comp. Physiol. A* **184**, 49–61 (1999).
20. Kumamota, E. & Shinnick-Gallagher, P. Slow inward and late slow outward currents induced by hyperpolarizing pre-pulses in cat bladder parasympathetic neurones. *Eur. J. Physiol.* **416**, 322–334 (1990).
21. Izhikevich, E. M. Neural excitability, spiking, and bursting. *Int. J. Bifurcat. Chaos* **10**, 1171–1266 (2000).
22. Kanold, P. O. & Manis, P. B. Transient potassium currents regulate the discharge patterns of dorsal cochlear nucleus pyramidal cells. *J. Neurosci.* **19**, 2195–2208 (1999).
23. Wu, M. & Jen, P. H.-S. Recovery cycles of neurons in the inferior colliculus, the pontine nuclei and the auditory cortex of the big brown bat, *Eptesicus fuscus*. *Chin. J. Physiol.* **41**, 1–8 (1998).
24. Westheimer, G. Discrimination of short time intervals by the human observer. *Exp. Brain Res.* **129**, 121–126 (1999).
25. Brand, A., Urban, A. & Grothe, B. Duration tuning in the mouse auditory midbrain. *J. Neurophysiol.* **84**, 1790–1799 (2000).
26. Peruzzi, D., Sivaramakrishnan, S. & Oliver, D. L. Identification of cell types in brain slices of the inferior colliculus. *Neurosci.* **101**, 403–416 (2000).
27. Sivaramakrishnan, S. & Oliver, D. L. Distinct K currents result in physiologically distinct cell types in the inferior colliculus of the rat. *J. Neurosci.* **21**, 2861–2877 (2001).
28. Hooper, S. L. Transduction of temporal patterns by single neurons. *Nature Neurosci.* **1**, 720–726 (1998).
29. Turrigiano, G., Abbott, L. F. & Marder, E. Activity changes the intrinsic properties of cultured neurons. *Science* **264**, 974–976 (1994).
30. Itoh, K. Stevens, B., Schachner, M. & Fields, R. D. Regulated expression of the neural cell adhesion molecule L1 by specific patterns of neural impulses. *Science* **270**, 1369–1372 (1995).
31. Fields, R. D., Eshete, F., Stevens, B. K. & Itoh, K. Action potential-dependent regulation of gene expression: temporal specificity in Ca^{+2}, cAMP-responsive element binding proteins, and mitogen-activated protein kinase signaling. *J. Neurosci.* **17**, 7252–7266 (1997).
32. Dolmetsch, R. E., Xu, K. & Lewis, R. S. Calcium oscillations increase the efficiency and specificity of gene expression. *Nature* **392**, 933–936 (1998).
33. Li, W., Llopis, J., Whitney, M., Zlokarnik, G., & Tsien, R. Y. Cell-permeant caged InsP$_3$ ester shows that Ca^{+2} spike frequency can optimise gene expression. *Nature* **392**, 936–941 (1998).
34. Muschol, M. & Salzberg, B. M. Dependence of transient and residual calcium dynamics on action-potential patterning during neuropeptide secretion. *J. Neurosci.* **20**, 6773–6780 (2000).
35. Hodgkin, A. L. & Huxley, A. F. A quantitative description of membrane current and its application to conduction and excitation in nerve. *J. Physiol. Lond.* **117**, 500–544 (1952).
36. Huguenard, J. R. & McCormick, D. A. A model of the electrophysiological properties of thalamocortical relay neurons. *J. Neurophysiol.* **68**, 1384–1400 (1992).